# New highly-percolating alginate-PEI membranes for efficient recovery of chromium from aqueous solutions

Yayuan Mo, Shengye Wang, Thierry Vincent, Jacques Desbrieres, Catherine Faur, Eric Guibal

# New highly-percolating alginate-PEI membranes for efficient recovery of chromium from aqueous solutions

Yayuan Mo[a], Shengye Wang[a,b], Thierry Vincent[a], Jacques Desbrieres[c], Catherine Faur[d], Eric Guibal[a,*]

[a] C2MA, IMT Mines Ales, Univ. Montpellier, Ales, France
[b] Department of Environmental Engineering, College of Chemistry and Environmental Engineering, Shenzhen University, PR China
[c] IPREM, UMR5254 – UPPA/CNRS, Technopole Helioparc, Pau, France
[d] IEM, Institut Européen des Membranes, Univ. Montpellier, CNRS, ENSCM, Montpellier, France

A B S T R A C T

Highly percolating membranes are prepared by the interaction of polyethylenimine and alginate (with glutaraldehyde crosslinking). SEM illustrates the macroporous structure of the material. The material is characterized by FTIR before and after chromate anions sorption. Batch-simulated continuous sorption experiments revealed that the maximum sorption occurred at pH 2 and the flow rate has limited effect on sorption efficiency. Uptake kinetics and sorption isotherms are well fitted by the pseudo-second-order rate and Sips equations, respectively. Maximum sorption is found close to 314 mg $g^{-1}$. Competition effects from Ca(II), Cu (II), $Cl^-$, $NO_3^-$, and $SO_4^{2-}$ are investigated to evaluate sorbent selectivity. The membranes are applied to remediate a simulate of Cr(VI) contaminated electroplating wastewater. Successive cycles of sorption and desorption show that the membranes maintain sorption capacity higher than 200 mg Cr $g^{-1}$ for both Cr(VI) and total chromium for the first two cycles. These new highly percolating membranes have promising performances for Cr(VI) removal.

*Keywords:*
Macroporous membranes
Alginate
Polyethyleneimine
Hexavalent chromium
Sorption isotherms
Uptake kinetics

## 1. Introduction

With the growing demand for chromium-based products and equipments, many industrial processes, such as electroplating, textile dyeing, petroleum refineries, leather tanning, wood preservation, and nuclear power plant, generate large amounts of chromium-contaminated wastewater (Setshedi, Bhaumik, Onyango, & Maity, 2015; Wang et al., 2015). In aqueous solutions, Cr mainly occurs under the most stable forms of trivalent Cr(III) cations (e.g., $Cr_2(OH)_2^{4+}$ and $Cr(OH)_2^{+}$) and hexavalent Cr(VI) anions (e.g., $HCrO_4^-$, $Cr_2O_7^{2-}$ and $CrO_4^{2-}$) (Konczyk, Kozlowski, & Walkowiak, 2010; Lytras et al., 2017). Cr(III) is an essential nutrient, at low concentrations, that plays an important role in the proper functioning of living organisms, while Cr(VI) is a highly toxic pollutant because of its teratogenicity, mutagenicity and carcinogenicity to living organisms even at ppb levels (Shanker, Cervantes, Loza-Tavera, & Avudainayagam, 2005; Xu et al., 2015). Therefore, removal of Cr(VI) from wastewater is very essential for protecting natural environment and human health.

Various methods such as chemical reduction (Ma et al., 2012), electrochemical precipitation (Kongsricharoern & Polprasert, 1996), ion exchange (Galán, Castañeda, & Ortiz, 2005), solvent extraction (Venkateswaran & Palanivelu, 2004), electrocoagulation (Aber, Amani-Ghadim, & Mirzajani, 2009), membrane filtration (Blöcher et al., 2003), sorption (Komárek, Koretsky, Stephen, Alessi, & Chrastný, 2015), etc. have been widely used for the removal of Cr(VI). The selection of the appropriate method is based on criteria such as the concentration of the metal ion, the pH of the solution, its complexity and the produced flow rates. Among these methods, sorption is a simple, efficient and low-cost technique and various sorbents such as abundant materials (e.g. activated carbon) (Ihsanullah et al., 2016), agricultural waste (Mahmood-ul-Hassan, Suthor, Rafique, & Yasin, 2015) and natural minerals (Thanos et al., 2017) have been investigated for the treatment of low-concentration effluents or as a polishing treatment. However, these sorbents may face several drawbacks including low stability and mechanical properties, difficulty in solid–liquid separation after treatment, generation of secondary pollution or cost-efficiency questions. To solve these problems, biosorbents have retained particular attention

* Corresponding author.
*E-mail addresses:* Yayuan.Mo@mines-ales.fr (Y. Mo), shengye.wang@szu.edu.cn (S. Wang), Thierry.Vincent@mines-ales.fr (T. Vincent), Jacques.Desbrieres@univ-pau.fr (J. Desbrieres), Catherine.Faur@umontpellier.fr (C. Faur), Eric.Guibal@mines-ales.fr (E. Guibal).

(Vijayaraghavan & Balasubramanian, 2015), including biopolymer matrices such as chitosan or alginate (Gopalakannan, Periyasamy, & Viswanathan, 2016; Sarode et al., 2018).

Alginate is a green, biocompatible and biodegradable polysaccharide that consists of blocks of 1–4 linked α-L-guluronic and β-D-mannuronic acids (Vu et al., 2017). It has been applied as an effective sorbent for heavy metals removal and a green encapsulating biopolymer for chemical and biological compounds; these applications are directly associated to the presence of numerous functional groups (e.g. carboxyl and hydroxyl) distributed along the backbone as coordination and reaction sites (Gopalakannan et al., 2016; Huang et al., 2018). For example, alginate was combined with chitosan (Gotoh, Matsushima, & Kikuchi, 2004), silica (Soltani, Khorramabadi, Khataee, & Jorfi, 2014), bentonite clay (Tan & Ting, 2014), cellulose (Lai, Thirumavalavan, & Lee, 2010), hydroxyapatite (Googerdchian, Moheb, & Emadi, 2012), graphene oxide (Jiao et al., 2016), maghemite particles (Idris, Ismail, Hassan, Misran, & Ngomsik, 2012) and polyethyleneimine (PEI) (Bertagnolli, Grishin, Vincent, & Guibal, 2016) to form new materials such as bead (Wang, Vincent, Faur, & Guibal, 2017b), magnetic composite (Lakouraj, Mojerlou, & Zare, 2014), aerogel (Jiao et al., 2016) and membrane (Chen, Liu, Hu, Ni, & He, 2011). The incorporation of these compounds contributes to enhancing its own mechanical properties and improving its sorption efficiency for the removal of heavy metals. Among them, PEI is a water-soluble polymer having abundant polar groups (amine group) and hydrophobic groups (vinyl group) that can combine with different materials. Meanwhile, it also can chelate heavy metal ions and has been widely applied for increasing the sorption capacities of modified sorbents (Saleh, Tuzen, & Sarı, 2017). Recently, Xiong, Wang, Chen, and Peng (2018) developed a recyclable sorbent for removal of anionic dyes from wastewater by assembling alginate and PEI onto magnetic microspheres. Sun, Chen, Su, Huang, and Dong (2016) prepared a novel sorbent (PEI/SA) by functionalizing PEI/sodium alginate with 3-aminopropyltriethoxysilane for the sorption of Cu(II) from aqueous solution. Moreover, our research group has also successfully prepared PEI-impregnated alginate-based beads. Their application to the sorption of palladium demonstrated high metal sorption capacity (Wang, Vincent, Faur, & Guibal, 2018), and also high stability after metal reduction for catalytic application (Wang, Vincent, Faur, Rodríguez-Castellón, & Guibal, 2019). Alternative conditionings have been designed for chitosan (Beppu, Arruda, Vieira, & Santos, 2004) and alginate (Li et al., 2017), including porous membranes, which could (a) increase the number of contact sites between sorbent and metal ions, and (b) keep highly percolating properties for sorption.

The rationale of this research consisted of evaluating the feasibility of designing highly percolating membranes (authorizing the feed of structured material with simple natural filtration, without pumping) with simple procedure, which does not require energy-consuming procedures for structuring the composite. The second objective of this work corresponded to evaluating the feasibility of using the as-prepared membranes for the recovery of chromate anions.

Therefore, this work investigates the sorption of Cr(VI) on this macroporous alginate-PEI membrane in a batch-like set-up: the membrane is disposed in a cylindrical holder and the solution is pumped through the membrane in a recirculation mode. The effect of pH on metal sorption, the uptake kinetics and the sorption isotherms are successively investigated (in terms of both quantification and modeling). FTIR spectroscopy and SEM-EDX analysis are also used for discussing the sorption mechanisms. It is noteworthy that a special attention is paid to the possible occurrence of reduction phenomena (Cr(VI) being readily reduced in acidic solutions, in the presence or organic compounds). The interference of other coexisting ions eventually present in the wastewater on the removal of Cr(VI) is investigated to evaluate the selective removal of Cr(VI). The suitability of the membranes is also evaluated with a (simulated) electroplating wastewater. At last, the desorption of Cr(VI) is carried out to test the reusability of membranes.

## 2. Materials and methods

### 2.1. Materials

The Cr(VI) and Cr(III) stock solutions were prepared by dissolving appropriate amounts of potassium dichromate ($K_2Cr_2O_7$) (Merck KGaA, Darmstadt, Germany) and chromium(III) chloride hexahydrate ($Cl_3Cr{\cdot}6H_2O$) (Sigma-Aldrich, Darmstadt, Germany) into 0.01 M HCl solution, respectively, then further diluted to obtain working solutions. All chemicals used in this study were of analytical grade and MilliQ water was used for preparing solutions. Alginate (commercial reference: Manugel GMB, Batch G1305601) was purchased from FMC BioPolymer (Ayr, UK), the ratio of mannuronic to guluronic acid (M/G) being 0.16/0.84 was determined by proton NMR. Water content in the sample was analyzed by DSC: 16.3% (w/w). The average molecular weight was determined by viscometry: 446,000 g/mol. The detailed procedures and results for alginate analysis are reported in Supplementary Information (SI).

An alginate solution (4%, w/w) was prepared by dissolving the exact quantity of alginate powder into water under vigorous stirring. A glutaraldehyde (GA) solution (50%, w/w) (Sigma-Aldrich, Saint-Louis, USA) was used as a crosslinking agent. The polyethyleneimine (branched PEI, 50%, w/w, Sigma-Aldrich, Saint-Louis, USA) was diluted with demineralized water (final weight concentration: 3%, w/w) and the pH was adjusted to the proper pH value (around 6.5), using $HNO_3$. All other pH adjustment was performed using HCl and NaOH solutions.

### 2.2. Membrane fabrication

Scheme S1 (see SI) shows the schematic process used for the synthesis of the macroporous membranes. The membrane was fabricated by diluting 132 g of 4% alginate solution with pure water to 500 g and stirring until obtaining a homogeneous solution. In a second step, 35 mL of 3% PEI solution was sequentially added to alginate solution (7 times: 5 mL every 10 s) under stirring. After 1 min of strong stirring the solution was rapidly poured into a rectangular mold. Fabricated membranes may have different sizes (thicknesses) by using different molds. The membrane was gradually formed by fully reacting PEI with alginate over 24 h. The third step consisted of crosslinking the membrane with glutaraldehyde to strengthen the material: 4 mL of GA (50%, w/w) were added into the mold with 300 mL demineralized water before immersing the membrane (which was previously carefully washed with deionized water four times) at room temperature. Finally, after 24 h of slow shaking (30 rpm) the membrane was carefully washed with deionized water before being air-dried for 2 days. The membrane was cut into circular specimens for the next experiments.

### 2.3. Physical characterization of percolating properties

The porosity of the membranes was obtained by pycnometer measurements using ethanol as the soaking agent, and measuring the total volume of membranes and the amount of ethanol required to fill the porous compartment (Eiselt, Yeh, Latvala, Shea, & Mooney, 2000; Wang, Hamza, Vincent, Faur, & Guibal, 2017).

The stability of the sorbents was measured by shaking the membrane disk in 20 mL of pure water for 72 h at 150 rpm. Then, the membranes were weighed after drying. Stability (%) was calculated as follows:

$$\text{Stability} = \frac{100 m_{eq}}{m_0} \quad (1)$$

where $m_0$ (mg) and $m_{eq}$ (mg) are the mass of the membrane disk before and after shaking.

The determination of the water flux through the membranes was conducted at 20 °C and 0.006 bar (calculated from the water height by $p = \rho g h$); the effective area of the membrane was 4.64 $cm^2$. The water

was maintained at the same level and the time consumed for passing 100 mL water though the membrane disk was recorded. The water flux ($J$, mL cm$^{-2}$ min$^{-1}$) was calculated by the following equation:

$$J = \frac{V_p}{A_t} \tag{2}$$

where $V_p$ (mL) is the permeate volume, $A$ (cm$^2$) the membrane effective area and $t$ (min) the time consumed.

In addition, the free draining flow velocity (free percolation without forced pumping) was determined by feeding water at the top of the column increasing flow rate. The limit flow rate for free draining corresponded to the beginning of water accumulation at the top of the membrane.

Experiments were repeated at least twice to evaluate the experimental error.

### 2.4. Characterization of sorbent

The pH point of zero charge ($pH_{PZC}$) corresponds to the pH of the solution surrounding the sorbents when the electrical charge density on a surface is zero. Therefore, the charges on the surface will be positive and negative when the pH is lower and higher than the $pH_{pzc}$, respectively. The $pH_{PZC}$ of the membranes was measured according to the pH-drift method (Lopez-Ramon, Stoeckli, Moreno-Castilla, & Carrasco-Marin, 1999; Wang, Vincent, Faur, & Guibal, 2017a). 50 mL of 0.1 M NaCl solution at different initial pH values ($pH_0$, in the range 2–10) were mixed with 0.1 g of membrane for 2 days under agitation (150 rpm) at room temperature. Then, the final pH ($pH_f$) was recorded and plotted against $pH_0$ and the $pH_{PZC}$ corresponds to the point at which $pH_f$ was equal to $pH_0$.

The surface morphology of the membrane and its changes after sorption were determined using SEM (Quanta FEG 200, Thermo Fisher Scientific, Mérignac, France). The main elemental analysis of the materials (semi-quantitative analysis) before and after Cr sorption was carried out using EDX accessory (Oxford Instruments France, Saclay, France). FTIR spectra were used to examine the functional groups of the membranes using an FTIR-ATR (Attenuated Total Reflectance tool) Bruker VERTEX70 spectrometer (Bruker, Germany) in the wavenumber range: 4000–400 cm$^{-1}$.

### 2.5. Sorption experiments

Batch sorption experiments were performed in a continuous treatment device (Scheme S2, see SI), in the recirculation mode, by pumping the metal-containing solution through a flow system composed of a peristaltic pump (Ismatec ISM404B, USA), filter membrane holders and water tanks. Different sizes of filter membrane holders can be selected depending on the diameter (Ø) of membrane disk used. In the process, the membrane disk has been fixed into the filter membrane holder, and the solution was pumped through the system on a recirculation mode at certain flow rate (i.e., 15 mL min$^{-1}$). Simultaneously, a gentle agitation was set under water tanks with a plate magnetic stirrer (Variomag Poly 15, Thermo, Germany). For the pH effect experiments, 50 mL of 200 mg L$^{-1}$ metal ion solutions at different pH values (in the range 0.5–4, adjusted with HCl or NaOH solution) were contacted with 30 mg of membrane (Ø: 12 mm; height: 4.0 ± 0.1 mm) for 2 days at room temperature, and the flow rate was maintained at 15 mL min$^{-1}$. For uptake kinetics, a piece of membrane (mass: 217 mg, Ø: 24.5 mm; height: 6.5 ± 0.1 mm) was contacted with 1 L of 100 mg L$^{-1}$ metal ion solutions at pH 2 at two different flow rates (15 mL min$^{-1}$ and 30 mL min$^{-1}$, respectively). Four milliliters of solution were collected at predetermined times and immediately filtered using filter papers (Ø 25 mm, Prat-Dumas, France). For the sorption isotherm, 30 mg of membrane were contacted with 50 mL of metal ion solution at different initial concentrations ($C_0$, ranging from 20 and 300 Cr mg L$^{-1}$) for 3 days at room temperature. The pH of the solutions was initially set at pH 2 and the flow rate maintained at 15 mL min$^{-1}$. For the effect of coexisting ions, such as $Ca^{2+}$, $Cu^{2+}$, $Cl^-$, $NO_3^-$, and $SO_4^{2-}$, which are commonly present in industrial effluents, 30 mg of macroporous membrane were contacted with 50 mL of Cr(VI) solution containing each of various components at different concentrations (ranging from 0 to 800 mg L$^{-1}$) for 3 days at room temperature. The concentrations of $SO_4^{2-}$ and $Ca^{2+}$ in electroplating and tannery effluent can reach up to 500 mg L$^{-1}$ and 800 mg L$^{-1}$, respectively (Gupta & Babu, 2009).

The concentration of Cr(VI) was analyzed using UV spectrophotometer (Varian 2050) at 540 nm by the diphenylcarbazide method, while the TCr (total chromium) concentration was determined by inductively coupled plasma atomic emission spectrometry (ICP-AES, JY Activa M, Jobin-Yvon, Horiba, Longjumeau, France) after proper dilutions. The Cr(III) concentration was then obtained by subtracting the amount of Cr(VI) from the TCr (i.e., TCr = Cr(III) + Cr(VI)). The solution pH was measured using a pH-meter cyber scan pH 6000 (Eutech Instruments, Nijkerk, The Netherlands).

For all these experiments, after filtration the samples were analyzed ($C_{eq}$, mg L$^{-1}$) and the mass balance equation was used for evaluating sorption performance. The removal percentage ($R$, %) and the sorption capacity ($q_{eq}$, mg g$^{-1}$) were calculated with Eqs. (3) and (4), respectively.

$$R\ (\%) = \frac{100(C_0 - C_{eq})}{C_0} \tag{3}$$

$$q_{eq} = \frac{(C_0 - C_{eq})V}{m} \tag{4}$$

where $V$ is the volume of solution (L) and $m$ the dry weight of membrane (g).

### 2.6. Simulated electroplating wastewater treatment

Actually, wastewater usually contains several metal ions (and inorganic anions), so in order to test the suitability of the macroporous membrane in a complex system, different masses (15 mg and 30 mg) of sorbents were applied to treat a synthesized electroplating wastewater and a single Cr-containing wastewater (control group). The synthesized wastewater was simulated from an electroplating unit at Kolkata, India, which contains 54.5 mg L$^{-1}$ of Cr(VI), 6.25 mg L$^{-1}$ of Cu(II), 26.4 mg L$^{-1}$ of Ca(II), 173.26 mg L$^{-1}$ of Na(I), 2.52 mg L$^{-1}$ of K(I) and 1.45 mg L$^{-1}$ of Zn(II) (Singha & Das, 2011). The synthesized solutions were treated at pH 2 for 2 days.

### 2.7. Desorption and reuse experiments

After the kinetic experiments at the flow rate of 15 mL min$^{-1}$, metal loaded membranes were washed with demineralized water. Four-mL sample was collected at predetermined times for analyzing residual metal concentration. For evaluating the reversibility of chromate-loaded membranes, the materials were subjected to desorption kinetic experiment using 1 L solution of NaOH at either 0.01 M (pH = 11.9) or 0.1 M (pH = 12.5) concentrations.

To determine the reusability of membranes, experiments on Cr(VI) sorption and desorption process were carried out for 3 cycles. For each cycle, 30 mg of macroporous membrane was contacted with 50 mL of 200 mg L$^{-1}$ Cr(VI) solution for 2 days and then desorbed for 4 h using 50 mL of 0.01 M NaOH solution (after optimization of desorption conditions). After each cycle of sorption–desorption, the membrane was washed by demineralized water four times for reuse in the next cycle.

The desorption efficiency (De, %) was calculated by the equation: De (%) = (amount of metal desorbed/amount of metal sorbed) × 100.

### 2.8. Modeling

In order to understand the dynamic process of metal ions sorption

**Table 1**
Modeling of uptake kinetics of Cr(VI) and TCr onto alginate/PEI membranes at two different flow rates (15 or 30 mL $min^{-1}$).

| Model | Parameter | $F$ = 15 mL $min^{-1}$ | | $F$ = 30 mL $min^{-1}$ | |
|---|---|---|---|---|---|
| | | Cr(VI) | TCr | Cr(VI) | TCr |
| | $q_{eq,exp}$ (mg $g^{-1}$) | 300.9 | 293.6 | 304.1 | 293.5 |
| PFORE | $q_{eq,cal}$ (mg $g^{-1}$) | 291.8 | 287.8 | 266.8 | 265.6 |
| | $k_1 \times 10^3$ ($min^{-1}$) | 1.6 | 1.6 | 1.5 | 1.7 |
| | $R^2$ | 0.732 | 0.705 | 0.696 | 0.743 |
| PSORE | $q_{eq,cal}$ (mg $g^{-1}$) | 303.0 | 294.1 | 303.0 | 294.1 |
| | $k_2 \times 10^5$ (g $mg^{-1}$ $min^{-1}$) | 2.4 | 2.4 | 2.8 | 3.1 |
| | $R^2$ | 0.993 | 0.993 | 0.994 | 0.995 |

onto membranes, the experimental sorption kinetics were linearly fitted with two common kinetic models, namely pseudo-first order rate equation (PFORE) and pseudo-second order rate equation (PSORE). Furthermore, three non-linear forms of isotherm models including Freundlich, Langmuir and Sips were used to describe the equilibrium experimental data (see below).

### 2.9. Statistical analysis

Selected experiments were duplicated and the calculated average values and standard deviations were embodied in the figures. In order to test the repeatability of the sorption performance of membranes, three identical membranes were fabricated at different times and used to remove Cr(VI). Their results are shown in Fig. S1 (see SI).

## 3. Results and discussion

### 3.1. Characterization of materials

#### 3.1.1. Percolation characteristics

The basic properties of the membranes are shown in Table 1. The porosity of the membrane reaches up to 93.4 ( ± 0.73)%; this is relatively high compared to chitosan/poly(vinyl alcohol) foams, as reported by Wang, Chung, Lyoo, and Min (2006). This is a favorable property for practical application in continuous sorption in simple percolation mode. The stability of membranes reaches 94.0 ( ± 0.10)%; this means that the material has a high physical stability and maintains its integrity under a high-speed shaking in water. Taking into account that the preferred mode of application consists of immobilizing the membranes in a column set-up, it can be extrapolated that the static immobilization of the membranes in the column fully preserves the material. The water flux of membranes reaches up to 34 mL $cm^{-2}$ $min^{-1}$ at 0.006 bar; this clearly demonstrates the natural highly-percolating property of the sorbents compared to cellulose acetate/PEI microfiltration membranes with water flux of 10–50 mL $cm^{-2}$ $min^{-1}$ at 0.69 bar, as reported by Chen et al. (2004). The free draining flow velocity was found close to 0.62 m $h^{-1}$.

#### 3.1.2. SEM and SEM-EDX analysis

The cross-section morphologies and the distribution of the main elements in the membrane before and after Cr(VI) sorption are characterized by SEM-EDX (Fig. 1). The SEM images show the porous structure of the material; this is a very opened structure that explains the high porosity and permeability of the sorbent discs. The analysis of specific surface area from $N_2$ sorption (not shown) confirmed that the material has poor micro- and meso-porosity. Changing the drying process (using either freeze-drying or drying under supercritical $CO_2$ conditions) did not significantly increase the specific surface of the material: the order of magnitude remains around 1–5 $m^2$ $g^{-1}$. The material has a very large macro-porosity that makes the membrane very efficient for natural percolation (without applied pressure) but the specific surface area and porosity (under mesopore size) negligible.

The EDX spectrum presented in Fig. 1 for raw sorbent (before metal sorption) shows the presence of C and O elements (tracers of organic composition of the sorbent) but also K, Na and Cl elements (associated to the processes of alginate extraction and of shaping/synthesis). The EDX spectrum for the membrane after metal sorption confirms the presence of Cr ions on the sorbent. The obvious increase in percentage of O after Cr(VI) sorption might be attributed to the sorption of negatively charged chromate ions (e.g., $HCrO_4^-$). Cr elements were distributed densely and homogeneously in the whole mass of the sorbent. This also means that the reactive groups are homogeneously distributed in the material (Fig. S2, see SI).

#### 3.1.3. FTIR spectroscopy analysis

FTIR is an important technique to analyze the main bands corresponding to the functional groups of the membranes. The raw membranes, the membranes after contacting with 200 mg $L^{-1}$ Cr(VI) at pH 2.0 and the membranes after desorption by 0.01 M NaOH were analyzed by FTIR-ATR spectroscopy (in the range of 4000–400 $cm^{-1}$). The FTIR spectra and the assignments of the main bands are reported in Fig. 2 and Table S1 (see Supplementary Material), respectively. For raw membrane (Fig. 2a), the main peaks are identified at 3243 $cm^{-1}$ (N—H and O—H stretching vibrations, including their overlapping) (Zhang, Chen, Zhang, & Wang, 2017), 2928 $cm^{-1}$ (C—H stretching) (Deng & Ting, 2005a; Naebe et al., 2014), 1592 $cm^{-1}$ (N—H bending and C=N vibration) (Abolmaali, Tamaddon, & Dinarvand, 2013; Lindén et al., 2015; Rahaman, Ghosh, Lu, & Ghosh, 2005), 1402 $cm^{-1}$ ($COO^-$ symmetric stretching) (Katti, Sikdar, Katti, Ghosh, & Verma, 2006; Kuila & Ray, 2014; Mandal & Ray, 2013), 1315 $cm^{-1}$ (C—N stretching vibration) (Mishra et al., 2010; Zhang, Pei, & Wang, 2009; Zhang, Ping, Ding, Cheng, & Shen, 2004), 1087 $cm^{-1}$ and 1028 $cm^{-1}$ (C—O stretching vibration) (Esmaeili & Khoshnevisan, 2016; Lawrie et al., 2007), and 947 $cm^{-1}$ (C—H deformation) (Bhaumik, Maity, Srinivasu, & Onyango, 2011).

After sorption reaction, the main changes are associated to the broad peaks between 3000 $cm^{-1}$ and 3500 $cm^{-1}$ due to the stretching vibration of amine and hydroxyl (or their overlaps). The peaks at 2928 $cm^{-1}$ and 947 $cm^{-1}$ disappeared; assigned to C—H stretching and C—H deformation, respectively, this means that their neighbor reactive groups are involved in metal binding or that the sorption of Cr(VI), associated with a mechanism of reduction of Cr(VI) into Cr(III), induces the oxidation of some reactive groups (Bhaumik et al., 2011; Deng & Ting, 2005a; Naebe et al., 2014). The shift of the peak from 1592 $cm^{-1}$ to 1579 $cm^{-1}$ may be assigned to N—H bending (assigned to the primary amine groups of PEI) (Wang & Li, 2015) and C=N vibration (due to the formation of Schiff bases generated by the reaction between PEI and GA) (Rahaman et al., 2005). The intensity of the peak at 1402 $cm^{-1}$ decreases (this band is assigned to $COO^-$ symmetric stretching of the carboxylate groups in alginat (Thakur, Pandey, & Arotiba, 2016). The peak at 1315 $cm^{-1}$ assigned to C—N stretching (Chandramohan et al., 2008; Mishra et al., 2010; Zhang et al., 2009; Zhang, Zhang, Liu, & Robinson, 2004) and resulting from the interaction between amine groups of PEI and aldehyde groups of GA is shifted (with a decrease in its intensity). The intensities of the peaks at 1087 $cm^{-1}$ and 1028 $cm^{-1}$ (assigned to C—O skeletal stretching vibrations (Viswanathan, Sundaram, & Meenakshi, 2009; Zhang, Ping, et al., 2004)) also decrease. Therefore, the sorption of Cr(VI) involves interactions of the metal ions with hydroxyl and carboxylic groups on alginate and amine groups from PEI-GA. However, carboxyl and hydroxyl groups should not be involved in metal binding with chromate species (anions). This could be an indication that Cr(VI) was partially reduced to Cr(III) (probably by amine groups) and then sorbed through coordination with these groups. Indeed, Mohanty, Jha, Meikap, and Biswas (2006) also reported that the sorption of Cr(VI) onto *Eichhornia crassipes* took place on hydroxyl groups (characterized by FTIR analysis). Nakano, Takeshita, and Tsutsumi (2001) proposed that Cr(VI) was firstly

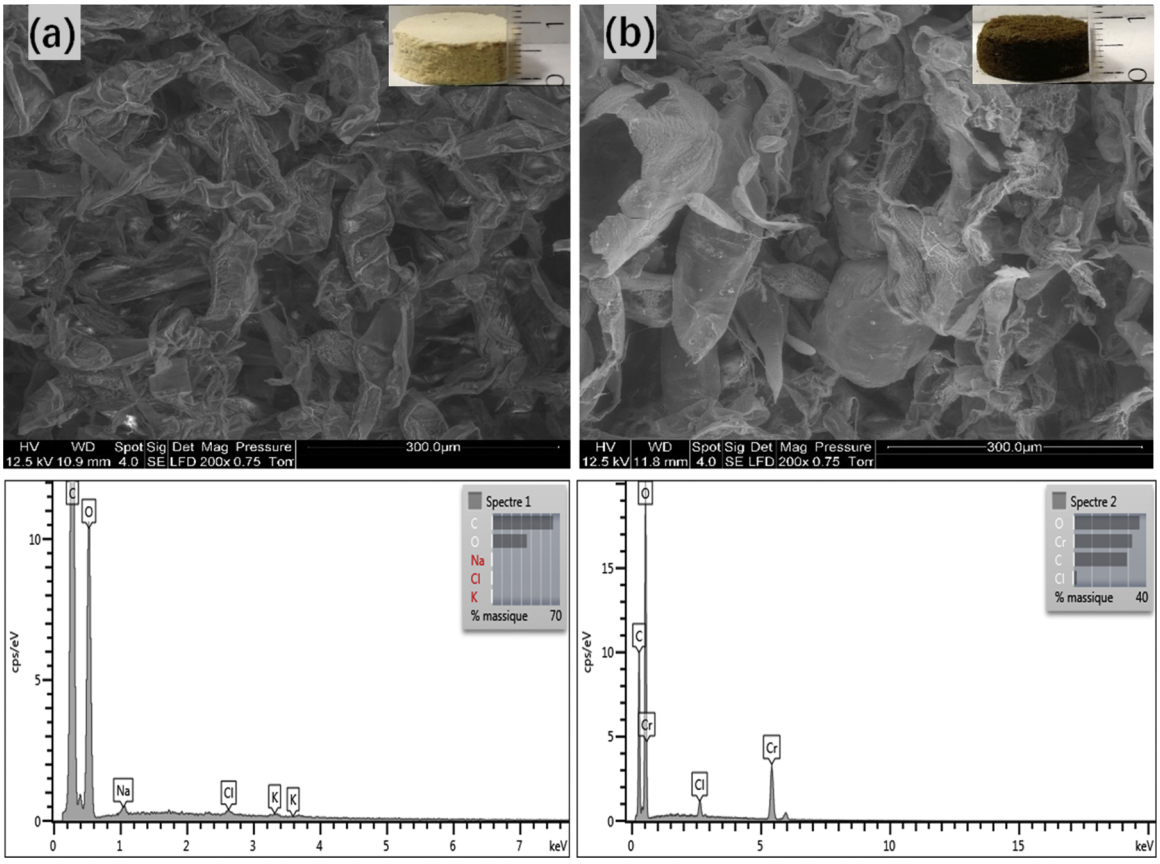


**Fig. 1.** SEM image and EDX analysis of membranes (a) before Cr sorption and (b) after Cr sorption.

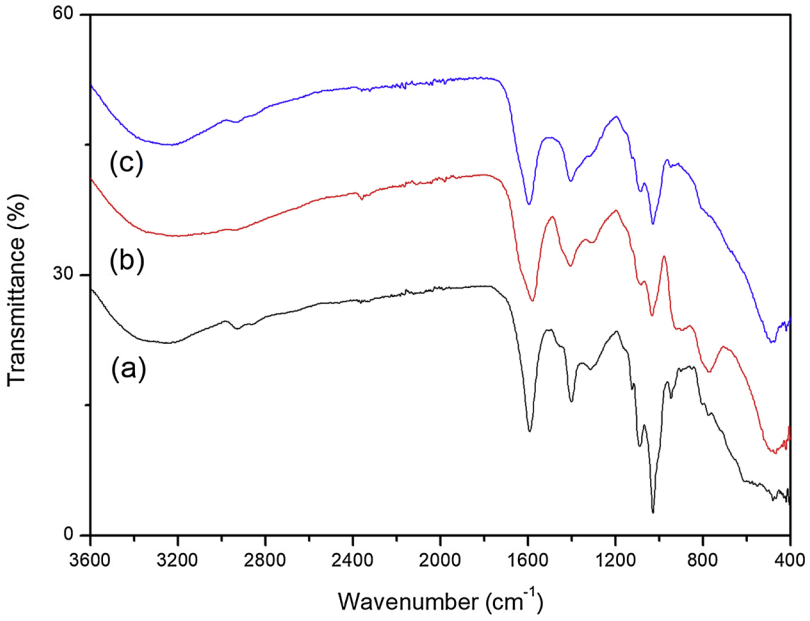


**Fig. 2.** FTIR spectra of membranes: (a) raw membrane; (b) membrane after Cr(VI) sorption; (c) membrane after metal desorption.

reduced to Cr(III) at low pH and then bound onto tannin gels through the ion exchange of Cr(III) with hydroxyl and/or carboxyl groups. Beside, a mechanism of electrostatic attraction between PEI on the membrane and chromate anions may be involved in Cr(VI) sorption, which was also reported by Yan, An, Xiao, Zheng, and Zhai (2017). Additionally, new peaks appeared at 895 $cm^{-1}$, 770 $cm^{-1}$ and 467 $cm^{-1}$ corresponding to the stretching vibrations of Cr═O, Cr—O and Cr—N, respectively; this further indicated that Cr(VI) was successfully sorbed on the membrane surface and the amine groups on PEI-GA play a major role in Cr(VI) binding (El-Medani, Ali, & Ramadan, 2005; Kalidhasan, Kumar, Rajesh, & Rajesh, 2012; Kumar et al., 2012; Kumar & Rajesh, 2013). The changes on the bands of reactive groups may also be explained by the protonation of reactive groups: carboxylate groups are fully protonated (carboxylic acid). However, the comparison of the

FTIR spectra for membranes conditioned under neutral and acidic solutions did not show substantial differences in the regions associated to carboxylate/carboxylic groups (not show).

After desorption, the FTIR spectrum goes back to the spectrum of raw membrane. Slight changes may be observed in the positions and intensities, but it did not change much compared to the raw membranes, except for the disappearance of the peak at 1315 $cm^{-1}$ (C—N stretching vibration) and for the presence of a peak in the range 450–550 $cm^{-1}$ (Cr—N stretching vibration). This is probably due to incomplete desorption of Cr. Based on the above analysis, the following possible mechanism of Cr(VI) sorption is proposed: (1) the sorption of Cr(VI) anions by amine groups from PEI-GA; (2) reduction of Cr(VI) to Cr(III) and (3) Cr(III) binding by coordination with hydroxyl and carboxylic groups.

In addition, the $pH_{PZC}$ of the sorbent is close to 5.73. The $pK_a$ values of carboxylic groups in alginate are usually reported at 3.38 and 3.65 for mannuronic acid and guluronic acid, respectively (Haug, 1961). On the other hand, PEI bears alkaline amine groups with different strengths (associated to primary, secondary and tertiary amine groups in branched polymer): $pK_a$ values are close to 7–8 and 10 (Ziebarth & Wang, 2009). This means that in the pH range selected for this study (i.e., 0.5–4) the overall charge of the sorbent is positive. The cationic behavior of the membrane opens the way for electrostatic attraction (ion-exchange mechanism) of anionic species (such as chromate anions) onto protonated groups.

### 3.2. Sorption properties

#### 3.2.1. Effect of pH

The pH is a critical operating parameter for sorption processes because of cross-effects on metal speciation and protonation/deprotonation of reactive groups (i.e., carboxylic groups, amine groups). In the case of Cr(VI), complementary mechanisms of reduction may also influence the interaction of the sorbent with metal ions (both in terms of sorption and desorption) (Sun et al., 2014). Several studies reported that the removal efficiency of Cr(VI) was higher for biosorbents at low pH (Aigbe, Das, Ho, Srinivasu, & Maity, 2018; Miretzky & Cirelli, 2010). In this work, the effect of pH on the sorption of Cr(VI) and TCr by alginate/PEI membranes was investigated in the pH range of 0.5–4; Fig. 3 shows a synthesis of these results. The optimum pH is reached at pH 2 under selected experimental conditions.

It is noteworthy that for most of pH values the curves for Cr(VI) and TCr overlap, except for pH 0.5. It is well known that the presence of organic matter at low pH causes the reduction of Cr(VI) into Cr(III). Chromate ion has a high positive redox potential and easily reduces in the presence of electron donors (Deng & Ting, 2005b). Several studies

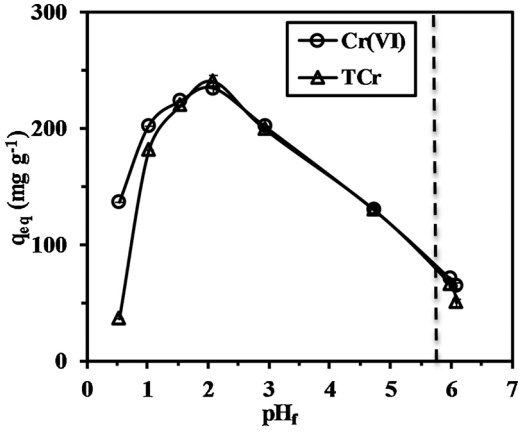


**Fig. 3.** Effect of pH on the sorption of Cr(VI) and TCr onto alginate/PEI membrane ($C_0$: 200 mg $L^{-1}$; $V$: 50 mL; sorbent mass: 30 mg; contact time: 48 h; flow rate: 15 mL $min^{-1}$; temperature: 20 ± 1 °C).

have shown that algal biomass sorbents can be used for the conversion of Cr(VI) into Cr(III) in acidic solution (Guha, Jayachandran, & Maurrasse, 2003; Park, Yun, & Park, 2004). At this low pH value, the reduction of Cr(VI) plays an important role and the cationic charge of Cr(III) is not favorable for binding on protonated reactive groups of the sorbent (both carboxylic and amine groups are protonated). The sorption capacity for total chromium strongly decreases compared to Cr(VI) removal: the mass balance on TCr gives at pH 0.5 a sorption capacity close to 36 mg TCr $g^{-1}$. On the other hand, the mass balance equation (i.e., TCr = Cr(III) + Cr(VI)) assessed on Cr(VI) in the solutions shows a removal that combines metal binding but also conversion of Cr(VI) into Cr(III) and the deduced sorption capacity is artificially increased up to 140 mg Cr(VI) $g^{-1}$. The sorption capacity of Cr(III) using alginate/PEI membrane was specifically quantified at pH 2: Cr(III) is weakly bound (less than 1.2 mg Cr(III) $g^{-1}$). This confirms that the difference between the Cr(VI) and TCr at pH 0.5 is essentially due to the proper reduction of the metal.

The $pH_{PZC}$ of the membrane is close to 5.73; this means that the reactive groups are strongly protonated at pH 4 (and below). These protonated groups can only bind anionic species (Zhou et al., 2016). At very low pH the strong protonation and the high concentration of counter anions (dissociation of the acid used for pH control) strongly compete with chromate anions for binding on carboxylic acids and more specifically on protonated amine groups. As the pH increases the surface remains positively charged but the competition effect of counter anions progressively decreases. However, above pH 2 the sorption capacity tends to decrease. This is directly attributed to the decrease in the protonation of amine groups, which, in turn, decreases the electrostatic attraction of chromate anions. Indeed, Guo, An, Xiao, Zhai, and Shi, 2017) reported that when the solution pH > 2 ($C_0$: 100 mg $L^{-1}$), the degree of protonation of $–NH_2$ decreased, resulting in a decrease in the sorption capacity of chromium(VI) onto PEI-functionalized cellulose aerogel beads. On the other hand, as the pH increases the global cationic charge decreases and at pH 4 the carboxylic groups are partially converted into carboxylate: their anionic charges may contribute to the particle repulsion of anionic species (or, at least, to moderate the attraction of these anionic metal species by protonated amine groups). As a matter of fact, pH 2 is good compromise between attractive effects on chromate anions and repulsive effects of counter anions of the acid media.

This means that another criterion is involved in the control of sorption. The speciation of chromate is a critical parameter for explaining the affinity of the sorbent for the metal. Fig. S3 (see Supplementary Material) shows the speciation of chromate ($C_0$: 200 mg Cr $L^{-1}$) as a function of pH (calculated with the Visual Minteq software (Gustafsson, 2013)). In the selected pH range (i.e., 0.5–4) the predominant species are $HCrO_4^-$ (between 75% and 87%) and $Cr_2O_7^{2-}$ (about 12%). At pH below 1, a neutral species $H_2CrO_4$ also appears (representing about 13%). Apart of the competitor effect of counter anions (from acid), the formation of neutral species contributes to the decrease in sorption properties. Similar research result has also been found in Cr(VI) removal by magnetic cellulose nanocomposite (Samuel et al., 2013). Therefore, pH 2 is the optimum pH value; further experiments were performed at this pH.

In addition, the values of initial pH ($pH_i$) and final pH ($pH_f$) after Cr (VI) sorption were recorded: the pH variation is non-negligible (Fig. S4, see SI). The $pH_f$ hardly changes at $pH_i$ below 2, while the $pH_f$ increases significantly as the $pH_i$ increased from 2.5 to 4.0: the largest variation was observed at $pH_i$ 3.5 (increased by 2.5 pH units). Finally, the $pH_f$ was stable and close to 6.0 in the range of pH 3.5–4, which revealed the pH buffering effect of the membrane.

#### 3.2.2. Uptake kinetics

Uptake kinetics allows fixing the equilibrium time but also to evaluating the steps that are controlling the transfer of the solute from the solution to the sorbent surface (Reddad, Gerente, Andres, & Le

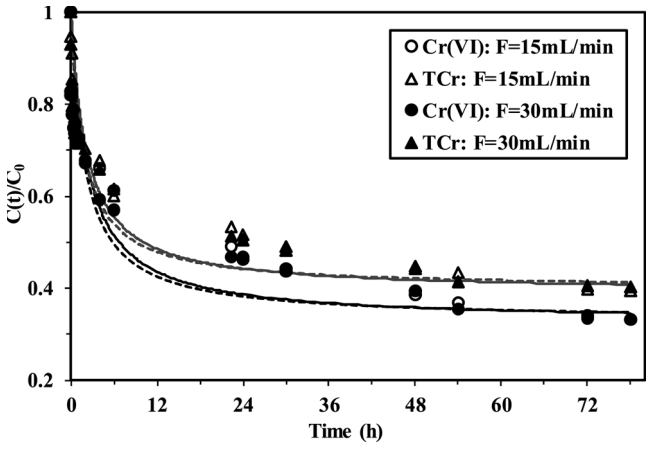


**Fig. 4.** Cr(VI) and TCr uptake kinetics using alginate/PEI membranes – effect of flow rate ($C_0$: 200 mg $L^{-1}$; $V$: 1 L; sorbent mass: 217 mg; pH: 2; contact time: 78 h; temperature: 20 ± 1 °C – lines represent the modeling of kinetic profiles with the pseudo-second order rate equation using parameters from Table 1).

Cloirec, 2002). Indeed, the sorption of metal ions can be controlled by different diffusion mechanisms (including bulk, film and intraparticle diffusions) and by the proper reaction rate (including parallel or complementary mechanisms of oxidation/reduction, precipitation). Fig. 4 shows the effect of flow rate (15 or 30 mL $min^{-1}$) on the uptake of Cr (VI) and TCr on the membrane at pH 2. Varying the flow rate (and then the superficial flow velocity) could affect the kinetic profiles. Indeed, the irregular distribution of the channels into the membrane could induce preferential channels and irregular distributions of flow transfer in the material. Forcing the flow rate at higher value may contribute to decrease the preferential channeling. The figure clearly shows that the flow rate does not significantly affect the concentration decay in the solution (at least in the range: 15–30 mL $min^{-1}$). The kinetic profiles show 3 steps in the process: (a) a fast initial stage (within the first hour of contact) represents 41 to 48% of total sorption, (b) a second slower phase (ranging between 1 and 6 h) corresponding to 58–66% of total sorption, and (c) a very slow sorption phase that lasts till 78 h. This long sequence means that the resistance to intraparticle diffusion is contributing to the overall control of the uptake kinetics.

In addition, the uptake kinetics of Cr(VI) and TCr have been modeled using the pseudo-first-order rate equation (PFORE, Eq. (5)) and the pseudo-second-order rate equation (PSORE, Eq. (6)) which are commonly used to describe the chemical reaction rates in homogeneous or heterogeneous systems (Reddad et al., 2002).

$$\ln(q_e - q_t) = \ln q_e - k_1 t \tag{5}$$

$$\frac{t}{qt} = \frac{1}{k_2 q_e^2} + \frac{t}{qe} \tag{6}$$

where $q_e$ (mg $g^{-1}$) and $q_t$ (mg $g^{-1}$) represent the sorption capacities of Cr(VI) at equilibrium and at time $t$ (min), respectively, and $k_1$ ($min^{-1}$) and $k_2$ (g $mg^{-1}$ $min^{-1}$) the apparent rate coefficients of PFORE and PSORE models, respectively.

The parameters of the models are summarized in Table 1. The linearization of the models is reported in Fig. S5 (see SI), respectively. According to the high determination coefficient $R^2$, the PSORE fits more appropriately the kinetic curves for Cr(VI) and TCr recovery by alginate/PEI membranes. In addition, the comparison of calculated and experimental values for the equilibrium sorption capacity systematically confirmed that the PFORE describes more realistically the experimental profile. The lines in Fig. 4 show the simulation of uptake kinetics with the PSORE and the parameters reported in Table 1. The model describes correctly the initial and final stages of the curves; however, there are some discrepancies in the intermediary stage (corresponding to the highest curvatures in the experimental profiles). The preference for the PSORE means that the sorption is surface reaction-controlled, with a chemical sorption involving valence forces through sharing or exchange of electrons between Cr(VI) or TCr and the sorbent.

### 3.2.3. Sorption isotherms

Sorption isotherms represent the equilibrium distribution of the solute between the liquid and solid phases at a fixed temperature (and pH). Playing with increasing concentration allows determining the maximum sorption capacity of the sorbent but also its affinity for target metal. The initial slope of the curve gives important information on this affinity and on the trend of the sorbent for reaching its saturation. The sorption isotherms are modeled by mechanistic (Langmuir equation) or empirical (Freundlich) equations. In most cases, the saturation plateau (finite sorption capacity) observed on sorption isotherms makes the Langmuir equation more appropriate for describing equilibrium distributions (Ng, Cheung, & McKay, 2002). However, in some cases involving several modes of interaction, different reactive groups, and other phenomena (such as local precipitation or condensation), the Langmuir model requires extensions (using muti-site sorption, or combination of Langmuir and Freundlich equations, such as the Sips equation). The Sips isotherm (also called the Langmuir-Freundlich isotherm) is a hybrid form of Langmuir and Freundlich equations. The Sips equation follows a trend similar to the Freundlich equation except that it reaches a finite saturation limit when the concentration is sufficiently high (Repo, Warchol, Kurniawan, & Sillanpää, 2010). The Langmuir, Freundlich and Sips equations were used to describe the Cr (VI) and TCr sorption isotherms (Foo & Hameed, 2010; Hokkanen, Bhatnagar, Repo, Lou, & Sillanpää, 2016):

Langmuir model: $$q_{eq} = \frac{b q_m C_{eq}}{1 + b C_{eq}} \tag{7}$$

Freundlich model: $$q_{eq} = k_f C_{eq}^{1/n} \tag{8}$$

Sips model: $$q_{eq} = \frac{k_s q_m C_{eq}^{1/n_s}}{1 + k_s C_{eq}^{1/n_s}} \tag{9}$$

where $C_{eq}$ (mg $L^{-1}$) represents the residual equilibrium concentration; $q_{eq}$ is the sorption capacity; $q_m$ (mg $g^{-1}$) is the maximum sorption capacity at saturation of the monolayer, $b$ (L $mg^{-1}$) is the Langmuir constant. The parameters $k_f$ and $n$ are the Freundlich constants, and $k_s$ and $n_s$ are the specific coefficients in the Sips equation.

Nonlinear regression analysis was used for fitting Eqs. (7)–(9). Experimental sorption isotherms (Fig. 5) were obtained, at pH 2, by variation of the initial chromate sorption between 20 and 300 mg Cr $L^{-1}$.

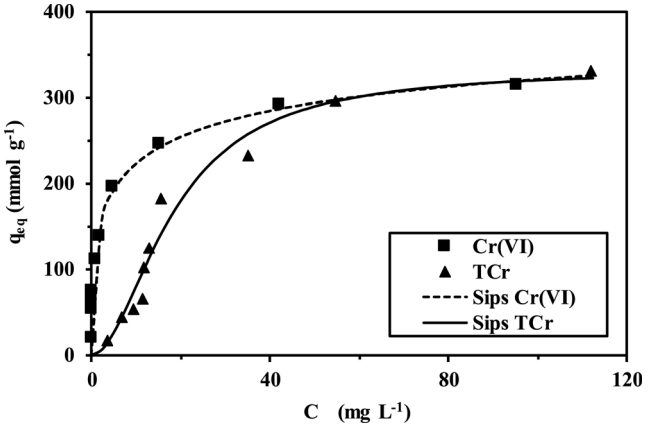


**Fig. 5.** Cr(VI) and TCr sorption isotherms on alginate/PEI membranes at pH 2 ($V$: 50 mL; sorbent mass: 30 mg; pH: 2; contact time: 78 h; flow rate: 15 mL $min^{-1}$; temperature: 20 ± 1 °C – lines represent the modeling of sorption isotherms with the Sips equation and the parameters summarized in Table 2).

**Table 2**
Sorption isotherms – Modeling parameters for Langmuir, Freundlich and Sips equations.

| Model | Parameter | Cr(VI) | TCr |
|---|---|---|---|
| Langmuir | $q_{m,exp}$ (mg g$^{-1}$) | 313.7 | 330.7 |
| | $q_{m,cal}$ (mg g$^{-1}$) | 297.9 | 480.7 |
| | $b$ (L mg$^{-1}$) | 0.539 | 0.024 |
| | $R^2$ | 0.884 | 0. 923 |
| Freundlich | $k_f$ (mg g$^{-1}$)/(L mg$^{-1}$)$^{1/n}$ | 130.4 | 27.02 |
| | $n$ | 4.885 | 1.803 |
| | $R^2$ | 0.968 | 0.851 |
| Sips | $q_{m,cal}$ (mg g$^{-1}$) | 455.3 | 332.4 |
| | ns | 2.521 | 0.529 |
| | $k_s$ | 0.383 | 0.004 |
| | $R^2$ | 0.987 | 0.954 |

The parameters of the models (together with their correlation coefficients) are reported in Table 2.

The sorption isotherm for Cr(VI) is characterized by a steep initial slope followed by the saturation plateau, which is reached for a residual concentration close to 40–50 mg Cr L$^{-1}$. This means that alginate/PEI membrane has a good affinity for chromate anions. Based on Table 2, it appears that Cr(VI) sorption isotherm follows both the Freundlich and the Sips equations, while the TCr sorption isotherm is better fitted by both the Langmuir and the Sips equations. Model fitting of the experimental data does not mean that the assumptions of the model are effectively verified but this may help for explaining the metal binding mechanism. The mathematical model designed by Freundlich accounts for describing multilayer sorption of Cr(VI) molecules, while Langmuir might be attributed to relatively homogeneous binding sites on the surface of the sorbents (Foo & Hameed, 2010).

Furthermore, the maximum sorption capacities of Cr(VI) and TCr reach 313.7 and 330.7 mg Cr g$^{-1}$, respectively (Table 2). These data showed relatively higher Cr(VI) sorption capacities, compared to most of reported sorbents (Table S2, see Supplementary Materials). Taking commercial resin as examples, Cr(VI) sorption capacities reached 89.3 and 126.6 mg Cr g$^{-1}$ for Purolite CT-275 and Purolite MN-500 ion-exchange resins, respectively (Baran, Bıçak, Baysal, & Önal, 2007). Xiao, Xu, Jiang, Dan, and Duan (2016) also reported a sorption capacity value in the range 105–120 mg Cr g$^{-1}$ for a series of polystyrene resins (D201, D202, and D301) at initial Cr(VI) concentration of 500 mg L$^{-1}$ and pH 2.

### 3.2.4. Effect of coexisting ions

Industrial effluents often contain various other anions and cations coexisting with Cr(VI); these ions may compete with reactive groups at the surface of the sorbent, or change metal speciation. This competition may significantly decrease the sorption performance. In order to evaluate the stability of sorption performance in complex solutions, the sorption efficiency of alginate/PEI membranes for Cr(VI) (and TCr) was compared in the presence of increasing concentrations of anions (e.g., $Cl^-$, $NO_3^-$ and $SO_4^{2-}$) and cations (e.g., Cu(II) and Ca(II)) at pH 2. In this case, the surface groups of sorbents are strongly protonated and beneficial to bind anionic species, and the main chromate species are $HCrO_4^-$ (about 87%) and $Cr_2O_7^{2-}$ (about 12%) at pH 2. Fig. 6 shows that monovalent anions, such as chloride and nitrate anions, even in excess, have a rather limited effect on chromate sorption: even at concentration as high as 800 mg L$^{-1}$ the decrease in sorption efficiency does not exceed 2%. Hu, Chen, and Lo (2005) also reported that the competitive effect of chloride and nitrate anions on Cr(VI) sorption by magnetic nanoparticles can be ignored and suggested that the two anions are poor ligands, which showed a weaker binding affinity for Cr (VI) species (and a low sorption on protonated amine groups). On the opposite hand, sulfate anions have a strong impact on sorption performance: the decrease in sorption efficiency may reach up to 30% for Cr(VI) and 44% for TCr. Sulfate anions being divalent have a stronger affinity (compared to mono-anionic $HCrO_4^-$ species) for protonated amine groups; this may explain the stronger effect of sulfate anions on metal binding. Even with large concentration excess metal cations such as Ca(II) and Cu(II) hardly affect chromate sorption: the loss in sorption efficiency remains below 8%. This can be easily explained by the protonation of reactive groups (carboxylic groups vs. carboxylate; and protonated primary and secondary amine groups). These protonated groups have poor affinity for metal cations. The carboxylate and free amine groups would predominate at higher pH values (above 4); these conditions would be more favorable for the sorption of metal cations, which, in turn, would have a greater effect on the sorption properties of the membranes. The alginate/PEI membranes have a remarkable selectivity for anionic metal ions in acidic solutions; on the contrary, the presence of competitor anions (counter anions, or anionic metal complexes) may be taken into account (especially when divalent).

### 3.2.5. Treatment of simulated electroplating wastewater

To test the suitability of the membranes in a complex system, alginate/PEI membrane was used to remediate a simulated electroplating wastewater. Table 3 presents the experimental data for the treatment of the wastewater; a single Cr-containing wastewater (containing a similar concentration of chromate) was used as control. The tests were performed using two different masses (15 mg and 30 mg) of alginate/PEI membrane. The $C_{eq}$ of Cr(VI) in the simulated electroplating wastewater and Cr-containing wastewater were 3.07 mg L$^{-1}$ and 2.66 mg L$^{-1}$, respectively, with a sorbent mass of 15 mg. While increasing the amount of sorbent to 30 mg, Cr(VI) was completely removed for the two solutions. The comparison of the results for the two wastewaters shows that the presence of other metal ions or anions in the solution hardly changes chromate binding and TCr removal. These conclusions are consistent with the results reported in the previous section. On the other hand, the analysis of total chromium (by ICP-AES) shows that chromium does not completely disappear from the solution because of the conversion of chromate into chromium(III), which is poorly sorbed on alginate/PEI membranes in acidic solutions. Moreover, the experimental results show that the sorbent has poor sorption capacities for other metal cations such as Cu(II), Ca(II), Na(I), K(I), and Zn(II). Alginate/PEI membranes have a great selectivity for chromate under selected experimental conditions. Therefore, the sorbent clearly demonstrates a great potential for removing Cr(VI) from industrial wastewater, as a polishing treatment.

### 3.2.6. Metal desorption and recycling of alginate/PEI membranes

Many previous studies have shown that NaOH solutions are highly efficient for desorbing Cr(VI) from loaded sorbents (Debnath, Maity, & Pillay, 2014; Hui, Chao, & Kot, 2005; Reddy, Chauhan, & Chakraborty, 2016). Fig. 7a shows the kinetic profiles for the desorption of chromate ions from Cr-loaded alginate/PEI membranes using 0.01 M and 0.1 M NaOH solutions. Increasing the concentration of the eluent increases the velocity of metal release: 1 h *vs.* 2 h for reaching the equilibrium. However, the concentration does not affect the effective desorption efficiency at equilibrium, which does not exceed 45%. It is noteworthy that during desorption experiments the released concentrations of Cr (VI) and TCr are equal (contrary to the observations made during sorption steps); this is obviously due to the different effects of chromate reduction during sorption (additional reduction on the sorbent) and desorption (no reduction).

The poor desorption of Cr(VI) is probably due to the partial reduction of Cr(VI) to Cr(III) during metal sorption on alginate/PEI sorption. This is consistent with FTIR analysis that showed an alteration of the biomass (remaining chromium but also partial degradation due to the oxidation of some reactive groups). Similar conclusions were reported in the case of chromate desorption from Cr-loaded mustard oil cake and polypyrrole/$Fe_3O_4$ magnetic nanocomposite (Bhaumik et al., 2011). As described above, the presence of organic matter at low pH

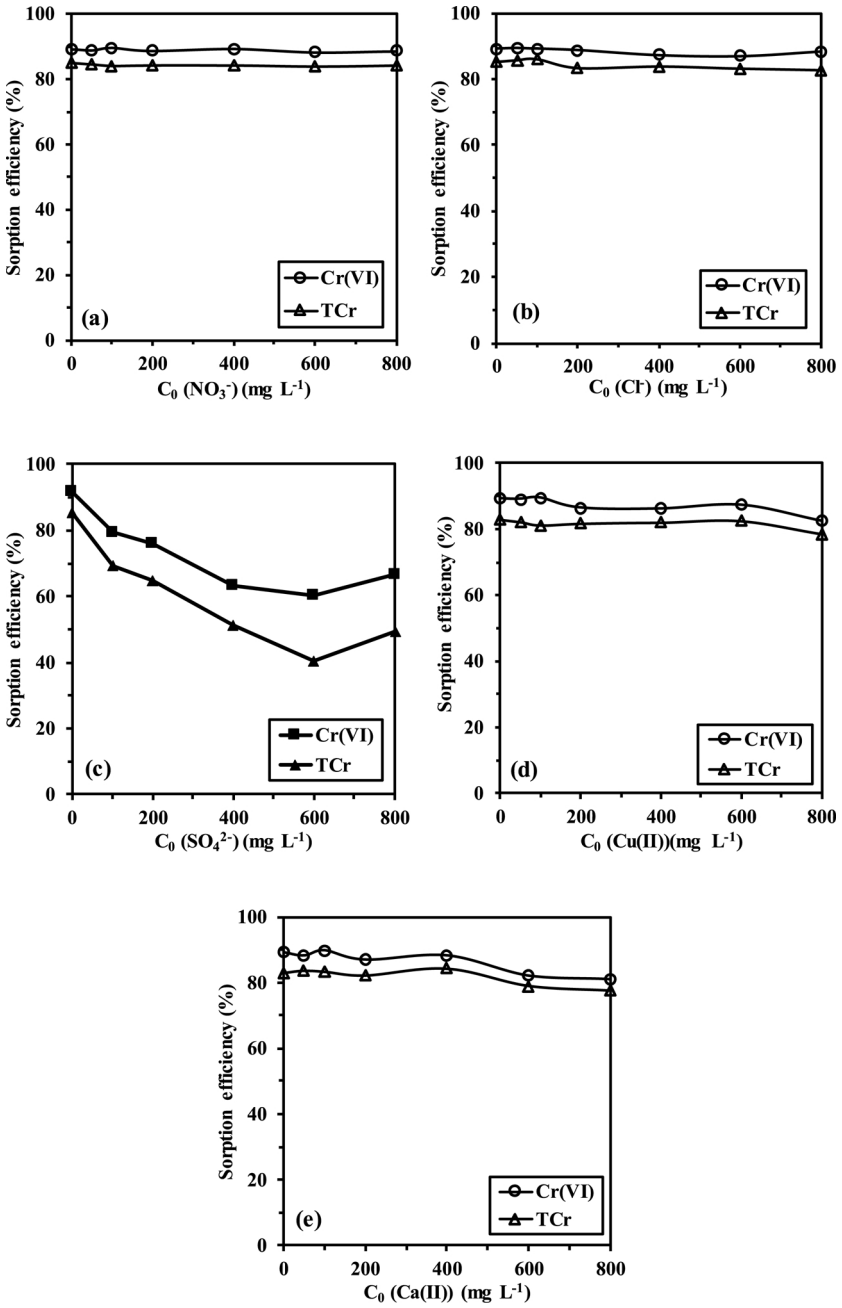


**Fig. 6.** Effect of coexisting ions on the removal of Cr(VI) and TCr by alginate/PEI membranes: (a) $NO_3^-$, (b) $Cl^-$, (c) $SO_4^{2-}$, (d) Cu(II) and (e) Ca(II) ($C_0$: 200 mg $L^{-1}$; $V$: 50 mL; sorbent mass: 30 mg; pH: 2; contact time: 72 h; flow rate: 15 mL $min^{-1}$; temperature: 20 ± 1 °C).

**Table 3**
Comparison of experimental data on the treatment of simulated electroplating wastewater and single Cr-containing wastewater (control group) at two different mass (15 mg and 30 mg) of membranes ($V$: 50 mL; pH: 2; contact time: 72 h; flow rate: 15 mL $min^{-1}$; temperature: 20 ± 1 °C).

| Waste-water | Simulated electroplating wastewaters | | | Single Cr-containing solution | | |
|---|---|---|---|---|---|---|
| | $C_0$ (mg $L^{-1}$) | Mass: 15 mg $C_{eq}$ (mg $L^{-1}$) | Mass: 30 mg $C_{eq}$ (mg $L^{-1}$) | $C_0$ (mg $L^{-1}$) | Mass: 15 mg $C_{eq}$ (mg $L^{-1}$) | Mass: 30 mg $C_{eq}$ (mg $L^{-1}$) |
| Cr(VI) | 53.4 | 3.07 ± 0.16 | 0.00 | 53.8 | 2.66 ± 0.10 | 0.00 |
| TCr | 55.6 | 8.93 ± 0.13 | 7.33 ± 0.44 | 55.9 | 7.01 ± 0.23 | 6.14 |
| Cu(II) | 6.71 | 6.65 ± 0.04 | 6.64 | – | – | – |
| Zn(II) | 1.16 | 1.09 ± 0.03 | 1.08 | – | – | – |
| Ca(II) | 26.5 | 26.5 | 26.5 | – | – | – |
| K(I) | 20.5 | 20.3 | 20.2 | – | – | – |
| Na(I) | 27.9 | 25.3 ± 0.48 | 24.7 | – | – | – |

$C_0$: metal initial concentrations; $C_{eq}$: metal residual equilibrium concentration.

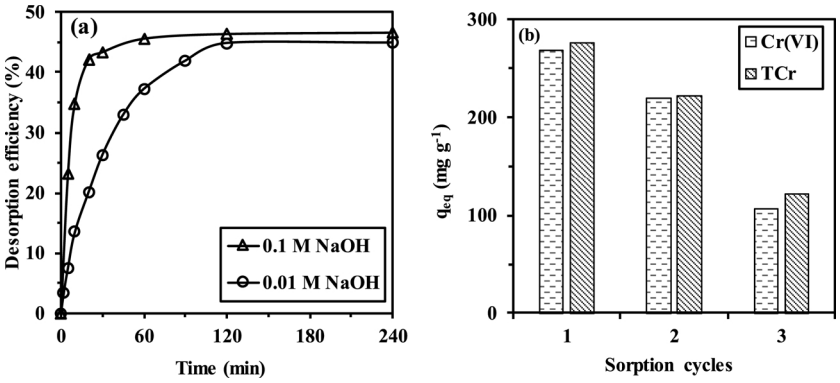


**Fig. 7.** Metal desorption from loaded alginate/PEI membranes and sorbent reycling: (a) desorption kinetics using solution of NaOH at 0.01 M (pH = 11.9) and 0.1 M (pH = 12.5) concentrations (Metal loading on the sorbent before desorption shown in Fig. 6. Desorption step – $V$: 1 L; time: 4 h; flow rate: 15 mL min$^{-1}$; temperature: 20 ± 1 °C) and (b) comparison of sorption–desorption performances for 3 successive cycles (sorption step – $C_0$: 200 mg L$^{-1}$; $V$: 50 mL; sorbent mass: 30 mg; pH: 2; contact time: 48 h; flow rate: 15 mL min$^{-1}$; temperature: 20 ± 1 °C. Desorption step – desorption agent: 0.01 M NaOH; $V$: 50 mL; time: 4 h; flow rate: 15 mL min$^{-1}$; temperature: 20 ± 1 °C).

causes the reduction of Cr(VI) into Cr(III), which may result in a decrease in desorption efficiency. Therefore, to test whether this was caused by the low pH (i.e., pH 2) during the sorption process, desorption of Cr-loaded membranes using 0.01 M NaOH after Cr(VI) sorption at pH 3 and 3.5 was also investigated. Relevant results are summarized in Table S3 (see Supplementary Material); they show that Cr (VI) desorption efficiency hardly changed when the pH used for sorption step was increased. This means that increasing the pH is supposed to reduce the yield of reduction on organic material, but does not affect the desorption efficiency in the present case.

Fig. 7b shows the comparison of sorption capacities for Cr(VI) and TCr under similar experimental conditions (sorption at pH 2 and desorption using 0.01 M NaOH solutions). The sorption capacity progressively decreases by 19% at the second cycle (sorption capacity remains as high as 219 mg Cr g$^{-1}$). However, at the third cycle, alginate/PEI membrane loses about 60% of its sorption capacity: residual capacity does not exceed 107 mg Cr g$^{-1}$. This value remains relatively high compared to the sorption capacities of other biosorbents. However, these data definitively show the difficulty to use this material for numerous cycles of sorption and desorption. The weak desorption of chromate hinders the re-use of the sorbent for more than 3 cycles.

## 4. Conclusions

Highly percolating membranes were successfully synthesized by dispersion of PEI in alginate solution and further cross-linking with GA. The highly macroporous membrane facilitates the percolation of water through the polymer network with high flow rates and limited loss of pressure. The presences of carboxylic groups (alginate matrix) and amine groups (primary, secondary and tertiary amines from PEI) bring to the composite material multi-functionality and affinity for a broad range of metal ions. In the case of chromate sorption from acid solutions, the sorption is mainly controlled by the protonation of amine groups that can selectively bind chromate anionic species. Unfortunately, under acidic conditions (i.e., pH 2), the composite membrane may be partially oxidized and chromate anions are partially reduced under the form of chromium(III). This strongly affects the possibility to desorb chromium from loaded membranes; this also limits the admissible number of cycles of sorption and desorption (no more than 3 cycles).

The uptake kinetics are poorly affected by the flow rate (for the recirculation of the solution – loop mode) but the time required for reaching equilibrium is quite long (about 3 days) though most of the sorption occurs within the first 24 h of contact. The pseudo-second order rate equation fits relatively well the kinetic profile, although the poor porosity at the surface probably controls the mass transfer (resistance to intraparticle diffusion). The sorption isotherms can be modeled using the Sips equation (for total chromium profile) or the Langmuir equation (for chromate profile). The maximum sorption capacities reach values as high as 314 mg Cr(VI) g$^{-1}$ and 331 mg TCr g$^{-1}$ at pH 2.

The sorption properties are poorly affected by the presence of chloride and nitrate anions or calcium and copper cations (even in large excess: 800 mg L$^{-1}$); however, the presence of sulfate ions shows a much greater impact with substantial depreciation of sorption capacities. Tested on simulated electroplating wastewater, alginate/PEI membranes reveal sorption capacities comparable to the levels reached with pure synthetic solutions. Finally, despite the efficiency in desorption is weak, the process sounds promising for the polishing treatment of such industrial effluents.

This study clearly confirms that the suggested procedure for synthesizing highly percolating membranes is successful: superficial flow velocities as high as 20 m h$^{-1}$ can be reached under pumping (with limited headloss: 6 mbar). The free draining flow velocity (without pumping) corresponds to 0.62 m h$^{-1}$. The simple air-drying procedure is sufficient for manufacturing highly macroporous material. The contribution of different modes of interaction of carboxylate and amine groups (mutual interactions, ionotropic gelation, crosslinking) may explain the stable structuration of the membrane during the air-drying step.

This study also demonstrates the highly efficiency of the new sorbent (which can be used in recirculation mode, but could also be used in the single-pass mode) for chromate removal: the material has outstanding sorption capacities compared to literature.

This is the first time to the best of our knowledge that such a composite material associating alginate with polyethyleneimine is described for synthesizing macroporous foams. This unique material makes profit of the presence of multiple interactions: (a) ionic interaction between carboxylic groups of alginate and amine groups of PEI, and (b) crosslinking of amine groups from PEI with glutaraldehyde. This is also the first time such a material with high macroporosity is synthesized without requiring a specific and sophisticated drying procedure (such as freeze-drying, cryogel manufacturing or drying under supercritical conditions).

## Acknowledgments

Y. Mo acknowledges the China Scholarship Council (CSC, Grant No. 201708450080) for providing PhD fellowship. S. Wang acknowledges the CSC (Grant No. 20156660002) for providing PhD fellowship. Authors thank Jean-Claude Roux (IMT Mines Alès, C2MA) for his technical support for SEM-EDX analyses. The contributions of Paola Alberny and Juliette Saviard (IMLT – Mines Ales engineering students) are also acknowledged for experimental support.

## References


Aber, S., Amani-Ghadim, A., & Mirzajani, V. (2009). Removal of Cr(VI) from polluted solutions by electrocoagulation: Modeling of experimental results using artificial neural network. *Journal of Hazardous Materials, 171*(1–3), 484–490.

Abolmaali, S. S., Tamaddon, A. M., & Dinarvand, R. (2013). Nano-hydrogels of methoxy polyethylene glycol-grafted branched polyethyleneimine via biodegradable cross-linking of $Zn^{2+}$-ionomer micelle template. *Journal of Nanoparticle Research, 15*(12), 2134.

Aigbe, U. O., Das, R., Ho, W. H., Srinivasu, V., & Maity, A. (2018). A novel method for removal of Cr(VI) using polypyrrole magnetic nanocomposite in the presence of unsteady magnetic fields. *Separation and Purification Technology, 194*, 377–387.

Baran, A., Bıçak, E., Baysal, Ş. H., & Önal, S. (2007). Comparative studies on the adsorption of Cr(VI) ions on to various sorbents. *Bioresource Technology, 98*(3), 661–665.

Beppu, M., Arruda, E., Vieira, R., & Santos, N. (2004). Adsorption of Cu(II) on porous chitosan membranes functionalized with histidine. *Journal of Membrane Science, 240*(1–2), 227–235.

Bertagnolli, C., Grishin, A., Vincent, T., & Guibal, E. (2016). Recovering heavy metal ions from complex solutions using polyethylenimine derivatives encapsulated in alginate matrix. *Industrial & Engineering Chemistry Research, 55*(8), 2461–2470.

Bhaumik, M., Maity, A., Srinivasu, V., & Onyango, M. S. (2011). Enhanced removal of Cr (VI) from aqueous solution using polypyrrole/$Fe_3O_4$ magnetic nanocomposite. *Journal of Hazardous Materials, 190*(1–3), 381–390.

Blöcher, C., Dorda, J., Mavrov, V., Chmiel, H., Lazaridis, N., & Matis, K. (2003). Hybrid flotation—membrane filtration process for the removal of heavy metal ions from wastewater. *Water Research, 37*(16), 4018–4026.

Chandramohan, A., Bharathikannan, R., Kandhaswamy, M., Chandrasekaran, J., Renganathan, R., & Kandavelu, V. (2008). Synthesis, spectral, thermal and NLO properties of *N,N*-dimethyl anilinium picrate. *Crystal Research and Technology: Journal of Experimental and Industrial Crystallography, 43*(2), 173–178.

Chen, J. H., Liu, Q. L., Hu, S. R., Ni, J. C., & He, Y. S. (2011). Adsorption mechanism of Cu (II) ions from aqueous solution by glutaraldehyde crosslinked humic acid-immobilized sodium alginate porous membrane adsorbent. *Chemical Engineering Journal, 173*(2), 511–519.

Chen, Z., Deng, M., Chen, Y., He, G., Wu, M., & Wang, J. (2004). Preparation and performance of cellulose acetate/polyethyleneimine blend microfiltration membranes and their applications. *Journal of Membrane Science, 235*(1–2), 73–86.

Debnath, S., Maity, A., & Pillay, K. (2014). Magnetic chitosan–GO nanocomposite: Synthesis, characterization and batch adsorber design for Cr(VI) removal. *Journal of Environmental Chemical Engineering, 2*(2), 963–973.

Deng, S., & Ting, Y.-P. (2005a). Characterization of PEI-modified biomass and biosorption of Cu(II), Pb(II) and Ni(II). *Water Research, 39*(10), 2167–2177.

Deng, S., & Ting, Y. P. (2005b). Polyethylenimine-modified fungal biomass as a high-capacity biosorbent for Cr(VI) anions: Sorption capacity and uptake mechanisms. *Environmental Science & Technology, 39*(21), 8490–8496.

Eiselt, P., Yeh, J., Latvala, R. K., Shea, L. D., & Mooney, D. J. (2000). Porous carriers for biomedical applications based on alginate hydrogels. *Biomaterials, 21*(19), 1921–1927.

El-Medani, S. M., Ali, O. A., & Ramadan, R. M. (2005). Photochemical reactions of group 6 metal carbonyls with N-salicylidene-2-hydroxyaniline and bis-(salicylaldehyde) phenylenediimine. *Journal of Molecular Structure, 738*(1–3), 171–177.

Esmaeili, A., & Khoshnevisan, N. (2016). Optimization of process parameters for removal of heavy metals by biomass of Cu and Co-doped alginate-coated chitosan nanoparticles. *Bioresource Technology, 218*, 650–658.

Foo, K. Y., & Hameed, B. H. (2010). Insights into the modeling of adsorption isotherm systems. *Chemical Engineering Journal, 156*(1), 2–10.

Galán, B., Castañeda, D., & Ortiz, I. (2005). Removal and recovery of Cr(VI) from polluted ground waters: A comparative study of ion-exchange technologies. *Water Research, 39*(18), 4317–4324.

Googerdchian, F., Moheb, A., & Emadi, R. (2012). Lead sorption properties of nanohydroxyapatite–alginate composite adsorbents. *Chemical Engineering Journal, 200*, 471–479.

Gopalakannan, V., Periyasamy, S., & Viswanathan, N. (2016). Synthesis of assorted metal ions anchored alginate bentonite biocomposites for Cr(VI) sorption. *Carbohydrate Polymers, 151*, 1100–1109.

Gotoh, T., Matsushima, K., & Kikuchi, K.-I. (2004). Preparation of alginate–chitosan hybrid gel beads and adsorption of divalent metal ions. *Chemosphere, 55*(1), 135–140.

Guha, H., Jayachandran, K., & Maurrasse, F. (2003). Microbiological reduction of chromium(VI) in presence of pyrolusite-coated sand by *Shewanella alga* Simidu ATCC 55627 in laboratory column experiments. *Chemosphere, 52*(1), 175–183.

Guo, D.-M., An, Q.-D., Xiao, Z.-Y., Zhai, S.-R., & Shi, Z. (2017). Polyethylenimine-functionalized cellulose aerogel beads for efficient dynamic removal of chromium(VI) from aqueous solution. *RSC Advances, 7*(85), 54039–54052.

Gupta, S., & Babu, B. (2009). Removal of toxic metal Cr(VI) from aqueous solutions using sawdust as adsorbent: Equilibrium, kinetics and regeneration studies. *Chemical Engineering Journal, 150*(2–3), 352–365.

Gustafsson, J. (2013). *Visual MINTEQ, Version 3.1*. Stockholm, Sweden: Division of Land and Water Resources, Royal Institute of Technology. http://www2.lwr.kth.se/English/Oursoftware/vminteq/download.html.

Haug, A. (1961). Dissociation of alginic acid. *Acta Chemica Scandinavica, 15*(4), 950–952.

Hokkanen, S., Bhatnagar, A., Repo, E., Lou, S., & Sillanpää, M. (2016). Calcium hydroxyapatite microfibrillated cellulose composite as a potential adsorbent for the removal of Cr(VI) from aqueous solution. *Chemical Engineering Journal, 283*, 445–452.

Hu, J., Chen, G., & Lo, I. M. (2005). Removal and recovery of Cr(VI) from wastewater by maghemite nanoparticles. *Water Research, 39*(18), 4528–4536.

Huang, Y., Wu, H., Shao, T., Zhao, X., Peng, H., Gong, Y., et al. (2018). Enhanced copper adsorption by DTPA-chitosan/alginate composite beads: Mechanism and application in simulated electroplating wastewater. *Chemical Engineering Journal, 339*, 322–333.

Hui, K., Chao, C. Y. H., & Kot, S. (2005). Removal of mixed heavy metal ions in wastewater by zeolite 4A and residual products from recycled coal fly ash. *Journal of Hazardous Materials, 127*(1–3), 89–101.

Idris, A., Ismail, N. S. M., Hassan, N., Misran, E., & Ngomsik, A.-F. (2012). Synthesis of magnetic alginate beads based on maghemite nanoparticles for Pb(II) removal in aqueous solution. *Journal of Industrial and Engineering Chemistry, 18*(5), 1582–1589.

Ihsanullah, Al-Khaldi, F. A., Abu-Sharkh, B., Abulkibash, A. M., Qureshi, M. I., Laoui, T., et al. (2016). Effect of acid modification on adsorption of hexavalent chromium (Cr (VI)) from aqueous solution by activated carbon and carbon nanotubes. *Desalination and Water Treatment, 57*(16), 7232–7244.

Jiao, C., Xiong, J., Tao, J., Xu, S., Zhang, D., Lin, H., et al. (2016). Sodium alginate/graphene oxide aerogel with enhanced strength–toughness and its heavy metal adsorption study. *International Journal of Biological Macromolecules, 83*, 133–141.

Kalidhasan, S., Kumar, A. S. K., Rajesh, V., & Rajesh, N. (2012). An efficient ultrasound assisted approach for the impregnation of room temperature ionic liquid onto Dowex $1\times 8$ resin matrix and its application toward the enhanced adsorption of chromium (VI). *Journal of Hazardous Materials, 213*, 249–257.

Katti, K. S., Sikdar, D., Katti, D. R., Ghosh, P., & Verma, D. (2006). Molecular interactions in intercalated organically modified clay and clay–polycaprolactam nanocomposites: Experiments and modeling. *Polymer, 47*(1), 403–414.

Komárek, M., Koretsky, C. M., Stephen, K. J., Alessi, D. S., & Chrastný, V. (2015). Competitive adsorption of Cd(II) Cr(VI), and Pb(II) onto nanomaghemite: A spectroscopic and modeling approach. *Environmental Science & Technology, 49*(21), 12851–12859.

Konczyk, J., Kozlowski, C., & Walkowiak, W. (2010). Removal of chromium(III) from acidic aqueous solution by polymer inclusion membranes with D2EHPA and Aliquat 336. *Desalination, 263*(1–3), 211–216.

Kongsricharoern, N., & Polprasert, C. (1996). Chromium removal by a bipolar electrochemical precipitation process. *Water Science and Technology, 34*(9), 109–116.

Kuila, S. B., & Ray, S. K. (2014). Separation of benzene–cyclohexane mixtures by filled blend membranes of carboxymethyl cellulose and sodium alginate. *Separation and Purification Technology, 123*, 45–52.

Kumar, A. S. K., Gupta, T., Kakan, S. S., Kalidhasan, S., Rajesh, V., & Rajesh, N. (2012). Effective adsorption of hexavalent chromium through a three center (3c) co-operative interaction with an ionic liquid and biopolymer. *Journal of Hazardous Materials, 239*, 213–224.

Kumar, A. S. K., & Rajesh, N. (2013). Exploring the interesting interaction between graphene oxide Aliquat-336 (a room temperature ionic liquid) and chromium(VI) for wastewater treatment. *RSC Advances, 3*(8), 2697–2709.

Lai, Y.-L., Thirumavalavan, M., & Lee, J.-F. (2010). Effective adsorption of heavy metal ions ($Cu^{2+}$, $Pb^{2+}$, $Zn^{2+}$) from aqueous solution by immobilization of adsorbents on Ca-alginate beads. *Toxicological and Environ Chemistry, 92*(4), 697–705.

Lakouraj, M. M., Mojerlou, F., & Zare, E. N. (2014). Nanogel and superparamagnetic nanocomposite based on sodium alginate for sorption of heavy metal ions. *Carbohydrate Polymers, 106*, 34–41.

Lawrie, G., Keen, I., Drew, B., Chandler-Temple, A., Rintoul, L., Fredericks, P., et al. (2007). Interactions between alginate and chitosan biopolymers characterized using FTIR and XPS. *Biomacromolecules, 8*(8), 2533–2541.

Li, Q., Li, Y., Ma, X., Du, Q., Sui, K., Wang, D., et al. (2017). Filtration and adsorption properties of porous calcium alginate membrane for methylene blue removal from water. *Chemical Engineering Journal, 316*, 623–630.

Lindén, J. B., Larsson, M., Kaur, S., Skinner, W. M., Miklavcic, S. J., Nann, T., et al. (2015). Polyethyleneimine for copper absorption II: Kinetics, selectivity and efficiency from seawater. *RSC Advances, 5*(64), 51883–51890.

Lopez-Ramon, M. V., Stoeckli, F., Moreno-Castilla, C., & Carrasco-Marin, F. (1999). On the characterization of acidic and basic surface sites on carbons by various techniques. *Carbon, 37*(8), 1215–1221.

Lytras, G., Lytras, C., Argyropoulou, D., Dimopoulos, N., Malavetas, G., & Lyberatos, G. (2017). A novel two-phase bioreactor for microbial hexavalent chromium removal from wastewater. *Journal of Hazardous Materials, 336*, 41–51.

Ma, H.-L., Zhang, Y., Hu, Q.-H., Yan, D., Yu, Z.-Z., & Zhai, M. (2012). Chemical reduction and removal of Cr(VI) from acidic aqueous solution by ethylenediamine-reduced graphene oxide. *Journal of Materials Chemistry, 22*(13), 5914–5916.

Mahmood-ul-Hassan, M., Suthor, V., Rafique, E., & Yasin, M. (2015). Removal of Cd, Cr, and Pb from aqueous solution by unmodified and modified agricultural wastes. *Environmental Monitoring and Assessment, 187*(2), 19.

Mandal, B., & Ray, S. K. (2013). Synthesis of interpenetrating network hydrogel from poly (acrylic acid-co-hydroxyethyl methacrylate) and sodium alginate: Modeling and kinetics study for removal of synthetic dyes from water. *Carbohydrate Polymers, 98*(1), 257–269.

Miretzky, P., & Cirelli, A. F. (2010). Cr(VI) and Cr(III) removal from aqueous solution by raw and modified lignocellulosic materials: A review. *Journal of Hazardous Materials, 180*(1–3), 1–19.

Mishra, R., Kumar, R., Kumar, S., Majeed, J., Rashid, M., & Sharma, S. (2010). Synthesis and in vitro antimicrobial activity of some triazole derivatives. *Journal of the Chilean Chemical Society, 55*(3), 359–362.

Mohanty, K., Jha, M., Meikap, B., & Biswas, M. (2006). Biosorption of Cr(VI) from aqueous solutions by *Eichhornia crassipes*. *Chemical Engineering Journal, 117*(1), 71–77.

Naebe, M., Wang, J., Amini, A., Khayyam, H., Hameed, N., Li, L. H., et al. (2014). Mechanical property and structure of covalent functionalised graphene/epoxy nanocomposites. *Scientific Reports, 4*, 4375.

Nakano, Y., Takeshita, K., & Tsutsumi, T. (2001). Adsorption mechanism of hexavalent

chromium by redox within condensed-tannin gel. *Water Research, 35*(2), 496–500.
Ng, J., Cheung, W., & McKay, G. (2002). Equilibrium studies of the sorption of Cu(II) ions onto chitosan. *Journal of Colloid and Interface Science, 255*(1), 64–74.
Park, D., Yun, Y.-S., & Park, J. M. (2004). Reduction of hexavalent chromium with the brown seaweed *Ecklonia* biomass. *Environmental Science & Technology, 38*(18), 4860–4864.
Rahaman, S. H., Ghosh, R., Lu, T.-H., & Ghosh, B. K. (2005). Chelating N,N′-(bis (pyridin-2-yl) alkylidene) propane-1,3-diamine pseudohalide copper(II) and cadmium(II) coordination compounds: Synthesis, structure and luminescence properties of [M (bpap)(X)] $ClO_4$ and [M(bpap)$(X)_2$][M = Cu, Cd; X = $N_3^-$, $NCS^-$]. *Polyhedron, 24*(12), 1525–1532.
Reddad, Z., Gerente, C., Andres, Y., & Le Cloirec, P. (2002). Adsorption of several metal ions onto a low-cost biosorbent: Kinetic and equilibrium studies. *Environmental Science & Technology, 36*(9), 2067–2073.
Reddy, T. V., Chauhan, S., & Chakraborty, S. (2016). Adsorption isotherm and kinetics analysis of hexavalent chromium and mercury on mustard oil cake. *Environmental Engineering Research, 22*(1), 95–107.
Repo, E., Warchol, J. K., Kurniawan, T. A., & Sillanpää, M. E. (2010). Adsorption of Co(II) and Ni(II) by EDTA-and/or DTPA-modified chitosan: Kinetic and equilibrium modeling. *Chemical Engineering Journal, 161*(1–2), 73–82.
Saleh, T. A., Tuzen, M., & Sarı, A. (2017). Polyethylenimine modified activated carbon as novel magnetic adsorbent for the removal of uranium from aqueous solution. *Chemical Engineering Research and Design, 117*, 218–227.
Samuel, J., Pulimi, M., Paul, M. L., Maurya, A., Chandrasekaran, N., & Mukherjee, A. (2013). Batch and continuous flow studies of adsorptive removal of Cr(VI) by adapted bacterial consortia immobilized in alginate beads. *Bioresource Technology, 128*, 423–430.
Sarode, S., Upadhyay, P., Khosa, M., Mak, T., Shakir, A., Song, S., et al. (2018). Overview of wastewater treatment methods with special focus on biopolymer chitin-chitosan. *International Journal of Biological Macromolecules, 121*, 1086–1100.
Setshedi, K. Z., Bhaumik, M., Onyango, M. S., & Maity, A. (2015). High-performance towards Cr(VI) removal using multi-active sites of polypyrrole–graphene oxide nanocomposites: Batch and column studies. *Chemical Engineering Journal, 262*, 921–931.
Shanker, A. K., Cervantes, C., Loza-Tavera, H., & Avudainayagam, S. (2005). Chromium toxicity in plants. *Environment International, 31*(5), 739–753.
Singha, B., & Das, S. K. (2011). Biosorption of Cr(VI) ions from aqueous solutions: Kinetics, equilibrium, thermodynamics and desorption studies. *Colloids and Surfaces B: Biointerfaces, 84*(1), 221–232.
Soltani, R. D. C., Khorramabadi, G. S., Khataee, A., & Jorfi, S. (2014). Silica nanopowders/alginate composite for adsorption of lead(II) ions in aqueous solutions. *Journal of the Taiwan Institute of Chemical Engineers, 45*(3), 973–980.
Sun, X., Chen, J. H., Su, Z., Huang, Y., & Dong, X. (2016). Highly effective removal of Cu (II) by a novel 3-aminopropyltriethoxysilane functionalized polyethyleneimine/sodium alginate porous membrane adsorbent. *Chemical Engineering Journal, 290*, 1–11.
Sun, X., Yang, L., Li, Q., Zhao, J., Li, X., Wang, X., et al. (2014). Amino-functionalized magnetic cellulose nanocomposite as adsorbent for removal of Cr(VI): Synthesis and adsorption studies. *Chemical Engineering Journal, 241*, 175–183.
Tan, W. S., & Ting, A. S. Y. (2014). Alginate-immobilized bentonite clay: Adsorption efficacy and reusability for Cu(II) removal from aqueous solution. *Bioresource Technology, 160*, 115–118.
Thakur, S., Pandey, S., & Arotiba, O. A. (2016). Development of a sodium alginate-based organic/inorganic superabsorbent composite hydrogel for adsorption of methylene blue. *Carbohydrate Polymers, 153*, 34–46.
Thanos, A. G., Katsou, E., Malamis, S., Drakopoulos, V., Paschalakis, P., Pavlatou, E. A., et al. (2017). Cr(VI) removal from aqueous solutions using aluminosilicate minerals in their Pb-exchanged forms. *Applied Clay Science, 147*, 54–62.
Venkateswaran, P., & Palanivelu, K. (2004). Solvent extraction of hexavalent chromium with tetrabutyl ammonium bromide from aqueous solution. *Separation and Purification Technology, 40*(3), 279–284.
Vijayaraghavan, K., & Balasubramanian, R. (2015). Is biosorption suitable for decontamination of metal-bearing wastewaters? A critical review on the state-of-the-art of biosorption processes and future directions. *Journal of Environmental Management, 160*, 283–296.
Viswanathan, N., Sundaram, C. S., & Meenakshi, S. (2009). Removal of fluoride from aqueous solution using protonated chitosan beads. *Journal of Hazardous Materials, 161*(1), 423–430.
Vu, H. C., Dwivedi, A. D., Le, T. T., Seo, S.-H., Kim, E.-J., & Chang, Y.-S. (2017). Magnetite graphene oxide encapsulated in alginate beads for enhanced adsorption of Cr(VI) and As(V) from aqueous solutions: Role of crosslinking metal cations in pH control. *Chemical Engineering Journal, 307*, 220–229.
Wang, H., Yuan, X., Wu, Y., Chen, X., Leng, L., Wang, H., et al. (2015). Facile synthesis of polypyrrole decorated reduced graphene oxide–$Fe_3O_4$ magnetic composites and its application for the Cr(VI) removal. *Chemical Engineering Journal, 262*, 597–606.
Wang, J., & Li, Z. (2015). Enhanced selective removal of Cu(II) from aqueous solution by novel polyethylenimine-functionalized ion imprinted hydrogel: Behaviors and mechanisms. *Journal of Hazardous Materials, 300*, 18–28.
Wang, S., Hamza, M. F., Vincent, T., Faur, C., & Guibal, E. (2017). Praseodymium sorption on *Laminaria digitata* algal beads and foams. *Journal of Colloid and Interface Science, 504*, 780–789.
Wang, S., Vincent, T., Faur, C., & Guibal, E. (2017a). Algal foams applied in fixed-bed process for lead(II) removal using recirculation or one-pass modes. *Marine Drugs, 15*(10), 315.
Wang, S., Vincent, T., Faur, C., & Guibal, E. (2017b). Modeling competitive sorption of lead and copper ions onto alginate and greenly prepared algal-based beads. *Bioresource Technology, 231*, 26–35.
Wang, S., Vincent, T., Faur, C., & Guibal, E. (2018). A comparison of palladium sorption using polyethylenimine impregnated alginate-based and carrageenan-based algal beads. *Applied Science, 8*(2), 264.
Wang, S., Vincent, T., Faur, C., Rodríguez-Castellón, E., & Guibal, E. (2019). A new method for incorporating polyethyleneimine (PEI) in algal beads: High stability as sorbent for palladium recovery and supported catalyst for nitrophenol hydrogenation. *Materials Chemistry and Physics, 221*, 144–155.
Wang, X., Chung, Y. S., Lyoo, W. S., & Min, B. G. (2006). Preparation and properties of chitosan/poly(vinyl alcohol) blend foams for copper adsorption. *Polymer International, 55*(11), 1230–1235.
Xiao, K., Xu, F., Jiang, L., Dan, Z., & Duan, N. (2016). The oxidative degradation of polystyrene resins on the removal of Cr(VI) from wastewater by anion exchange. *Chemosphere, 156*, 326–333.
Xiong, B., Wang, N., Chen, Y., & Peng, H. (2018). Self-assembly of alginate/polyethyleneimine multilayer onto magnetic microspheres as an effective adsorbent for removal of anionic dyes. *Journal of Applied Polymer Science, 135*(7), 45876.
Xu, S., Pan, S., Xu, Y., Luo, Y., Zhang, Y., & Li, G. (2015). Efficient removal of Cr(VI) from wastewater under sunlight by Fe(II)-doped $TiO_2$ spherical shell. *Journal of Hazardous Materials, 283*, 7–13.
Yan, Y., An, Q., Xiao, Z., Zheng, W., & Zhai, S. (2017). Flexible core-shell/bead-like alginate@ PEI with exceptional adsorption capacity, recycling performance toward batch and column sorption of Cr(VI). *Chemical Engineering Journal, 313*, 475–486.
Zhang, C., Ping, Q., Ding, Y., Cheng, Y., & Shen, J. (2004a). Synthesis, characterization, and microsphere formation of galactosylated chitosan. *Journal of Applied Polymer Science, 91*(1), 659–665.
Zhang, J., Chen, S., Zhang, H., & Wang, X. (2017). Removal behaviors and mechanisms of hexavalent chromium from aqueous solution by cephalosporin residue and derived chars. *Bioresource Technology, 238*, 484–491.
Zhang, X., Pei, X., & Wang, Q. (2009). The tribological properties of acid-and diamine-modified carbon fiber reinforced polyimide composites. *Materials Chemistry and Physics, 115*(2–3), 825–830.
Zhang, X., Zhang, J., Liu, Z., & Robinson, C. (2004b). Inorganic/organic mesostructure directed synthesis of wire/ribbon-like polypyrrole nanostructures. *Chemical Communications, 16*, 1852–1853.
Zhou, L., Liu, Y., Liu, S., Yin, Y., Zeng, G., Tan, X., et al. (2016). Investigation of the adsorption-reduction mechanisms of hexavalent chromium by ramie biochars of different pyrolytic temperatures. *Bioresource Technology, 218*, 351–359.
Ziebarth, J. D., & Wang, Y. (2009). Understanding the protonation behavior of linear polyethylenimine in solutions through Monte Carlo simulations. *Biomacromolecules, 11*(1), 29–38.